

Medical Image Retrieval Based on Shape Features in DCT Domain

Ling Xia*, Zhi Peng, AnDong Cai, Haibin Wang

School of Electrical and Information Engineering, Xihua University, China

*Corresponding author, e-mail: xialing.cd@gmail.com

Abstract

Compressed medical images are widely used in clinical teaching and diagnosis. To save computing cost and storage spaces, research on compressed medical image retrieval is meaningful. This paper proposes a novel medical image retrieval scheme in DCT (Discrete Cosine Transformation) compressed domain. We firstly obtain the multi resolution image by reorganizing the DCT coefficients, then, segment the medical image's ROI (Region of Interest) and acquires the shape binary image in DCT compressed domain. We use Hu invariant moments to extract shape feature vectors, and measure the similarity by weighting method. Experiments were carried out on an image database which contains 1000 medical CT images. The experimental results show that this algorithm can correctly extract shape features of ROI and get good retrieval performance on JPEG medical images.

Keywords: medical image retrieval, shape features, DCT compressed domain, DCT coefficients, ROI

Copyright © 2014 Institute of Advanced Engineering and Science. All rights reserved.

1. Introduction

Human society has been advanced into the information era. With image data dramatically increasing, the development of image retrieval technology is getting faster and faster. Original image retrieval method is the Text-Based Image Retrieval (TBIR), which label the keywords and obtain demand images via retrieving these keywords. TBIR method is simple, fast and easy, but image information is huge and is of abundant content, the keywords are hard to be properly described and exactly abstracted in many situations [1]. In the beginning of 1990s, the technology of Content-Based Image Retrieval (CBIR) turned up. This method uses basic vision features, such as color, shape, texture, brightness structure. It does not need much anthropic intervention and annotation, it automatically analyses image features and accomplishes retrieval. CBIR technology develops rapidly and researchers have acquired many scientific achievements [2-5]. However, in order to save and transmit expediently, most images are compressed. To increase efficiency and performance, people begin to study the image retrieval in compressed domain, which retrieves the image under the situation of partly decompression or non-decompression [6]. Because there are a lot of image formats, such as JPEG (Joint Photographic Experts Group), H.261/H.263, MPEG-1/2, which are compressed by the way of DCT, the research on DCT compressed domain image retrieval is extremely meaningful. In recent years, there are some compressed domain image retrieval methods presented, for example, Lay presented an image retrieval method based on energy histograms of the low frequency DCT coefficients [7]; Lu proposed a content-based image retrieval scheme in JPEG compressed domain [8]; Lu and Burkhardt proposed a color image retrieval method based on DCT-domain vector quantization index histograms [9]; Hossein et al. used clustering techniques in DCT domain to object-based image retrieval [10]; Feng and Jiang presented a JPEG compressed image retrieval method via statistical features [11]. Reference [12] count the amount of Connected-Regions on the multi resolution image and establish Connected-Region Histogram as feature to do retrieval (we call this method as CRH-DCT algorithm).

With the development of medical imaging technology and popularization of hospital information network, medical image data play a important role in medical teaching, clinical diagnosis, patient situation tracking and medical research [13]. How to manage and use these resources is very essential. Therefore, medical image retrieval has become a very hot research

in the field of biomedicine engineering [14]. However, as we have known there has been little research on medical image retrieval in the DCT domain.

Considering JPEG medical images compressed by DCT transform take big proportion in real applications, this paper addressed on medical image retrieval in DCT compressed domain. Firstly, we acquire the DCT coefficients by partly decompression and get a multi resolution image, then, we segment medical image's ROI, after that, we do gray-level transformation and morphological processing to acquire a shape binary image of ROI, lastly we adopt Hu invariant moments to extract shape feature vectors and measure the similarity by weighted Euclidean distance. The flow chart of our algorithm is shown in Figure 1.

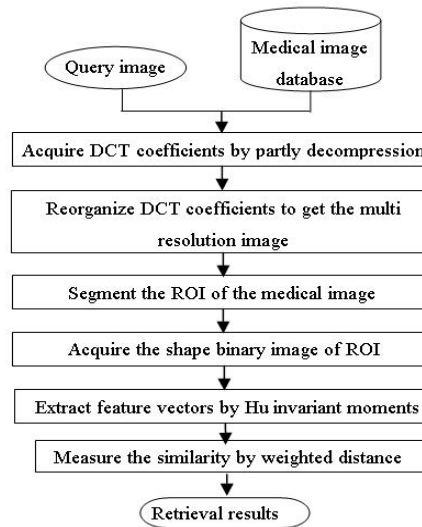


Figure 1. Flow Chart of Proposed Medical Image Retrieval System

2. Research Method

To explain what is DCT compressed domain image retrieval clearly, we draw a schematic diagram which is shown as Figure 2.

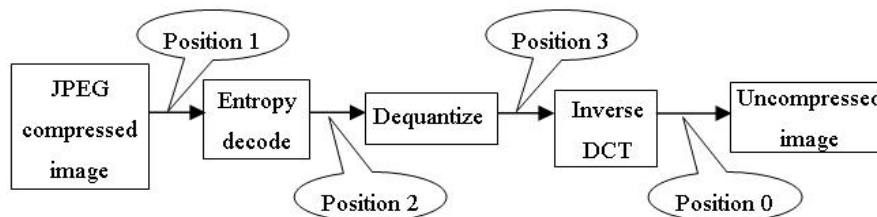


Figure 2. Flow Chart of JPEG Image Decompression

The decompression procedure of JPEG compressed image can be shown as Figure 2. Extracting features at position 1 is the retrieval in non-decompression situation, this kind of retrieval is hard to achieve. Extracting features at position 2 or 3 is the retrieval in the partly compressing situation. Extracting features at position 0 is pixel domain based image retrieval or general content based image retrieval [6].

2.1. Reorganization of DCT Coefficients

In this work, we acquire the DCT coefficients of the image by partly decompression, which is entropy decoding and de-quantizing to the JPEG image. See Figure 2, our DCT coefficients is acquired at position 3.

After getting DCT coefficients, the multi-resolution character can be constructed by referring to 3 scale wavelet decomposition. Figure 3 indicates an 8*8 image block of 3 scale wavelet decomposition and DCT coefficients division.

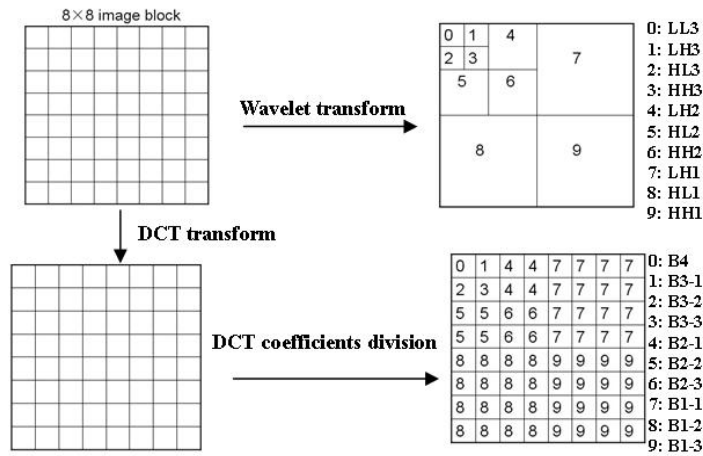


Figure 3. Divide DCT Coefficients Referring to 3 Scale Wavelet Decomposition

From Figure 3, we can see that we segment all DCT coefficients in an image into several 8*8 pixel image blocks, then, divide DCT coefficients in per 8*8 blocks into 10 areas just like 10 sub-bands of 3 scale wavelet decomposition: B4, B3-1, B3-2, ... B1-3, the number of coefficients are 1, 4, 16 respectively [12].

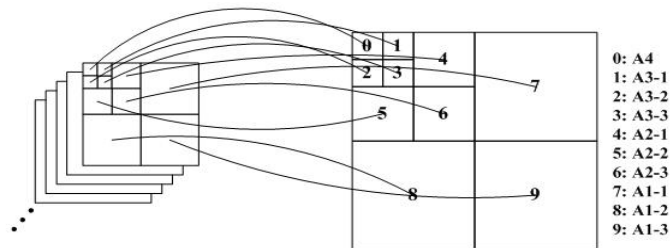


Figure 4. Reorganize DCT Coefficients of an Image

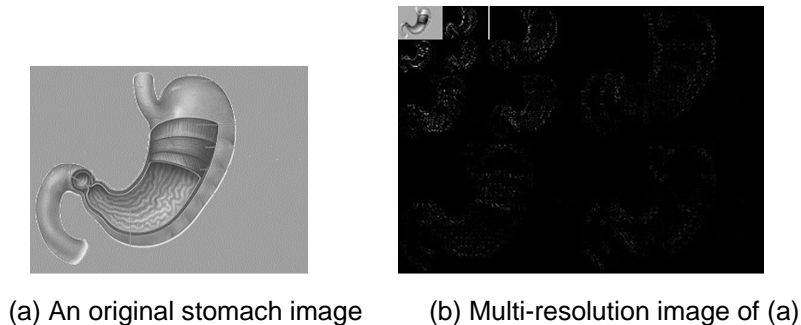


Figure 5. A Stomach Image and its Multi-resolution Image

Refer to Figure 3 and Figure 4, the next step is to get together the areas which are in the same position of each 8*8 image block. Namely, gather all B4 areas together as area A4, organize all

B3-1 areas together into area A3-1, , organize all B1-3 areas into area A1-3. After reorganizing DCT coefficients, the multi-resolution character of DCT compressed domain has been constructed and a multi-resolution image is obtained. Thus, A4 is the DC part of the image, Area A3 and A2 represent the low frequency components, the coefficients in A1 belong to high frequency of the image. For example, Figure 5(a) is an original stomach image, its multi-resolution image is shown in Figure 5(b).

From Figure 5(b) one can see that A4 area is a thumbnail of the whole image and represents the general visage. Area A1 has weak representability on original image, because it represents the subtle variety of the image content [15]. Coefficients in areas A3 and A2 represent the basic variety of the image content. We observed that areas A2 and A3 have stronger expressive ability on the shape of image ROI. Therefore, we choose A2 and A3 as the important areas for shape features extracting.

2.2. ROI Shape Features Extraction

a. ROI segmentation

In medical imaging applications, we are usually interested only in a certain area of an image, for example, an organ or a location of physiological structure, we call this kind of region as Region of Interest (ROI). The performance of ROI segmentation influences the effect of medical image retrieval, identification or classification.

To introduce the ROI segmentation method proposed in this work, take the area A2 in multi-resolution image as an example (area A3 will be processed in the same way). We combine area A2-1, A2-2, A2-3 into one area. The method can be described as: let (a, b) denotes the coordinate of the pixel; at the same coordinate point, A2-1, A2-2, A2-3 have a pixel value respectively. Comparing the 3 values, we can get the maximum value. By finding the maximum pixel values at all coordinate points and gathering them together, a new image block A2 (a, b) whose size is equal to A2-1 can be acquired. Figure 6 shows the A2 (a, b) image block of area A2 in a stomach multi-resolution image.

Formula 1 shows the construction and the expression of A2 (a, b) .

$$A2(a, b) = \max \{A2-1(a, b), A2-2(a, b), A2-3(a, b)\} \quad (1)$$



Figure 6. A2 (a, b) Image Block of Area A2

We investigated that the background of medical images usually is monotone. In most situations, the gray level distribution in the 4 corners of the medical image can represent the gray level distribution of the whole background. We also find pixel values are very close to each other among the background, these values are quite small and not equal to 0. According to this character, we use the following method to segment ROI from the A2 (a, b) image block:

(1) From each corner of A2 (a, b) image, a square area of 10×10 pixels is taken out.

(2) Convert gray level 0 to 255 into 85 gray units, that is, $[0,1,2,3), [3,4,5,6), [6,7,8,9), \dots, [252,253,254,255)$, it means that the interval between gray unit is 3 gray levels.

(3) For all pixels of the 4 square areas, distribute them into the 85 gray units according to their gray levels. Then find the gray unit which contains the most pixels and take the maximal value of the gray unit as threshold T.

(4) To all pixels in A2 (a, b) , set pixel values which are greater than T to value 1, set pixel values which are equal or less than T to value 0.

After the above process, ROI image can be obtained shown as Figure 7.



Figure 7. ROI Segmentation of Stomach Image

b. Morphological processing

Note that while segmenting the ROI, some over-segmentation and punctuate noise will happen (see Figure 7). To make the final shape binary image clearer, morphological processing is carried out. Take Figure 7 as an example, the first step is applying close-operation to shape binary ROI image I1 and obtaining image I2. The purpose of this operation is to fill up gaps in the contour, and make non-continuous edge continue. Then fill the holes in I2 to wipe off cavities. After filling process, image I3 is generated. Lastly, opening operation is conducted to I3 and final shape binary image I4 is obtained. Opening operation can not only smooth the edge but also wipe off punctuate noise. The morphological processing procedure is shown in Figure 8.

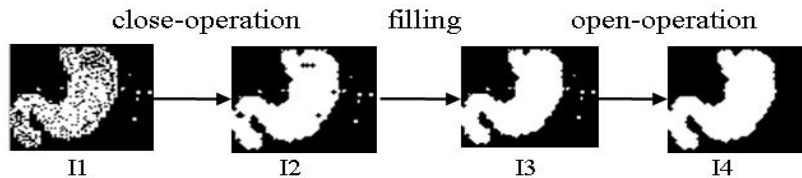


Figure 8. Morphological Processing of the ROI Image

c. Feature vector extraction

On the basis of the final shape binary image (see I4 in Figure 8), we extract shape features by Hu invariant moments. To construct the invariants, the basic terms are defined.

To image $f(x, y)$, the moment of order $(p+q)$ is defined as Formula 2:

$$m_{pq} = \sum_x \sum_y x^p y^q f(x, y) \quad p, q = 1, 2, \dots \quad (2)$$

Its corresponding central moments are defined as Formula 3:

$$\mu_{pq} = \sum_x \sum_y (x - \bar{x})^p (y - \bar{y})^q f(x, y) \quad p, q = 0, 1, 2, \dots \quad (3)$$

Where:

$$\bar{x} = m_{10} / m_{00}, \quad \bar{y} = m_{01} / m_{00}$$

The normalized central moments of order $(p+q)$ are denoted as Formula 4:

$$\eta_{pq} = \frac{\mu_{pq}}{\mu_{00}^\gamma} \quad p, q = 0, 1, 2, \dots \quad (4)$$

Where:

$$\gamma = \frac{p+q}{2} + 1 \quad \text{for } p+q = 2, 3, \dots \quad (5)$$

Hu constructed 7 invariant moments using normalized moments of order 2 and central moments of order 3, which are shown as formula 6 and formula 7. Hu invariant moments describes shape features of image content and has the advantage of invariant to translation, rotation, and scale change [16].

$$\left. \begin{aligned} I_1 &= \eta_{20} + \eta_{02} \\ I_2 &= (\eta_{20} - \eta_{02})^2 + 4\eta_{11}^2 \\ I_3 &= (\eta_{30} - 3\eta_{12})^2 + (3\eta_{21} - \eta_{03})^2 \\ I_4 &= (\eta_{30} + \eta_{12})^2 + (\eta_{21} + \eta_{03})^2 \\ I_5 &= (\eta_{30} - 3\eta_{12})(\eta_{30} + \eta_{12})I_x + (3\eta_{21} - \eta_{03})(\eta_{21} + \eta_{03})I_y \\ I_6 &= (\eta_{20} - \eta_{02}) \left[(\eta_{30} + \eta_{12})^2 - (\eta_{21} + \eta_{03})^2 \right] + 4\eta_{11}(\eta_{30} + \eta_{12})(\eta_{21} + \eta_{03}) \\ I_7 &= (3\eta_{21} - \eta_{03})(\eta_{30} + \eta_{12})I_x + (3\eta_{12} - \eta_{30})(\eta_{21} + \eta_{03})I_y \end{aligned} \right\} \quad (6)$$

Where:

$$\left. \begin{aligned} I_x &= (\eta_{30} + \eta_{12})^2 - 3(\eta_{21} + \eta_{03})^2 \\ I_y &= 3(\eta_{30} + \eta_{12})^2 - (\eta_{21} + \eta_{03})^2 \end{aligned} \right\} \quad (7)$$

Using Hu invariant moments to extract features from the shape binary image of ROI, we can get feature vectors. Then we do Gaussian normalization to get the normalized feature vector whose inside components have the same weight.

2.3. Similarity Measurement

After feature extraction, Euclidean distance between the query image and images in the database is used to measure the similarity in our system.

$$L(X, Y) = \sqrt{\sum_{i=1}^n (x_i - y_i)^2} \quad (8)$$

In Formula 8, $L(X, Y)$ is the Euclidean distance between two feature vectors X and Y , x_i and y_i stands for the No. i component in X and Y .

As discussed in section 2.1 we extracted shape features of ROI from both A2 and A3 area. We firstly calculate the Euclidean distances between the query and database for these two areas respectively (noted as L_{A2} and L_{A3}). Based on the ability to describe shape features of A2 and A3 areas, we use a weighting method to get the final distance L . The formula of distance calculation is shown in Formula 9. Where, the weighting factors 0.4 and 0.6 are chosen by plenty of experiments.

$$L = 0.4 * L_{A2} + 0.6 * L_{A3} \quad (9)$$

3. Retrieval Experiments and Discussion

The proposed algorithm has been implemented in the Matlab 2010 platform. Our database contains 1000 medical CT images of the JPEG format. Some examples in this database are shown in Figure 9. All images are preprocessed into the same size 300*256.

The database consists of different organs, body parts and imaging angle. A few images are obtained by means of translation, rotation, and scale change from the original images. According to the shape of image content, these CT images were divided into 10 categories shown as Figure 10.

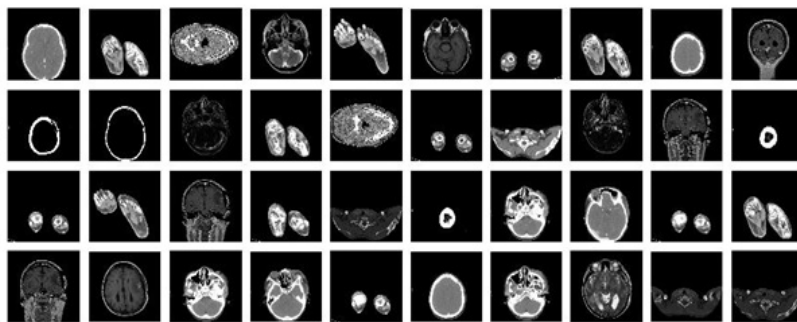


Figure 9. Examples of the Medical Image Database

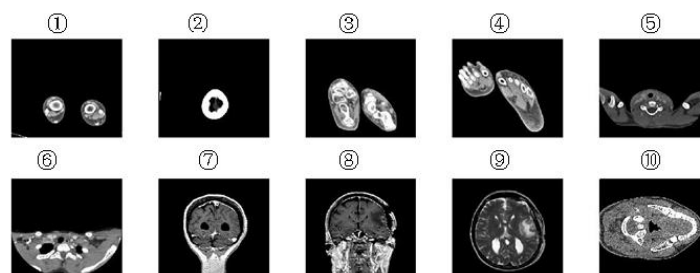
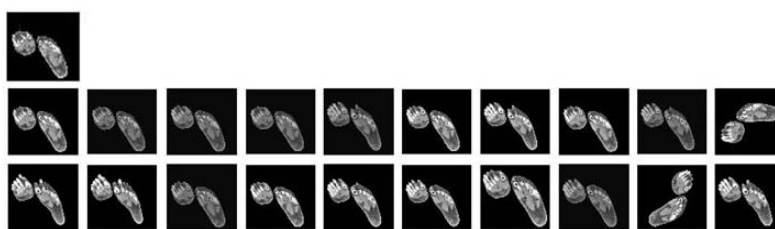


Figure 10. Example Images of the 10 Categories

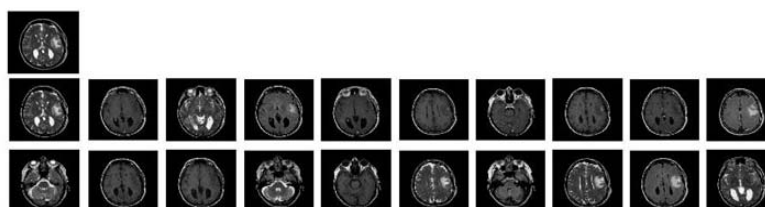
3.1. Medical Image Retrieval

Two query images are used here randomly to illustrate the retrieval performance of our algorithm as shown in Figure 11.

An image from category ③ is taken as query image, the retrieval results is given in Figure 11(a). Another query image is coming from category ⑨ and Figure 11(b) shows the retrieval results.



(a)



(b)

Figure 11. Two Retrieval Results using our Algorithm

3.2. Precision and Recall

Most common evaluation measures used in image retrieval are precision and recall [17]. We randomly take 3 images from each category as query images, namely, 30 images are taken from the 1000 images to do 30 times retrievals. For each query image we take down the precision value when the recall is respectively 10%, 20%, 30%, ,100%. Average precision values at each point of the 10 recall ratios for each category are shown in Table 1.

Table 1. Average Precision of 10 Recall Ratios for Each Category

recall → precision category ↓	10%	20%	30%	40%	50%	60%	70%	80%	90%	100%
①	100%	69.2%	70.1%	69.9%	68.9%	66.2%	66.7%	66.7%	62.3%	53.2%
②	100%	100%	100%	81.4%	60.9%	36.8%	10.3%	8.8%	6.8%	6.3%
③	100%	90.3%	77.6%	74%	72.3%	71%	63.1%	49.4%	43.7%	33.5%
④	100%	77.3%	61.7%	64.9%	62.7%	61.7%	61.5%	54.9%	48.5%	38.2%
⑤	81.9%	62.1%	61.2%	57.3%	56%	42.3%	42.5%	44.9%	44.3%	33.9%
⑥	100%	100%	100%	100%	100%	100%	100%	100%	97.4%	82.2%
⑦	85.2%	86.3%	81.7%	84.2%	85.3%	81.6%	77.2%	73.5%	63.6%	34.8%
⑧	100%	85.2%	83.9%	80.8%	78.2%	75.7%	71.9%	71.9%	63.2%	40.9%
⑨	100%	100%	100%	100%	94.2%	87.2%	85.7%	86%	84.2%	51.5%
⑩	100%	100%	93.3%	80.7%	82.1%	82.5%	78.3%	65%	61.1%	50.1%

To evaluate the overall system retrieval performance, we compute the average precision value at each point of the 10 recall ratios for all the 30 images to get an average PR curve as shown in Figure 12. In the same way, the CRH-DCT algorithm's average PR curve is acquired and also is shown in Figure 12.

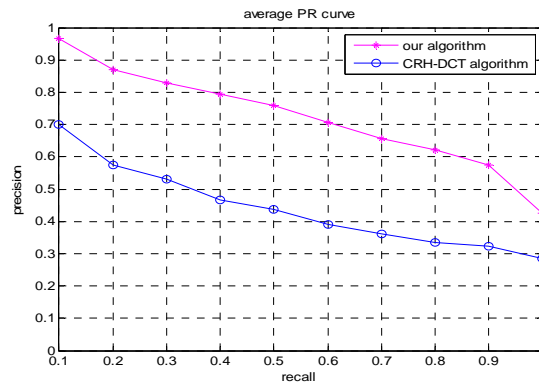


Figure 12. Average PR Curves of our Algorithm and CRH-DCT Algorithm

3.3. Discussion

Observing from Figure 11, all the images appear in the results is the same shape category with the query images. We noticed those images, which have the similar shape but have different positions, different scale and rotation angle with the query, also appear in the retrieval results. It is because that the Hu invariant moments has the advantage of invariant to translation, rotation, and scale change. In Figure 11, when query image is a brain image, 20 brain images are obtained in the retrieval result. But they have a different texture inside. If we want to distinguish different kinds of brain images, we should take texture as features to do further retrieval.

We use the average PR curve to evaluate the retrieval performance of our algorithm in depth. Table 1 shows that category 6 has the best retrieval performance, while category 2 has the lowest one. According to Figure 12, the average PR curve of our algorithm is obviously higher than the average PR curve of the CRH-DCT algorithm. Figure 12 also shows that our algorithm has a good retrieval capability in overall for medical CT images.

4. Conclusion

This work researched on medical image retrieval in the DCT compressed domain. After acquiring the multi-resolution image and segmenting the ROI of medical image, shape features were directly extracted in the DCT domain. To deal with the different effect of the DCT coefficients areas, we exploit the weighting method to measure the similarity. The experimental results show that our algorithm has a good retrieval capability for medical CT images. But if we need more elaborate retrieval, we should further pay attention to texture features.

Acknowledgements

This work was financially supported by the key research project of Xihua University (Z1120945), 2011 Chunhui program, Chinese Ministry of Education (Z2011090) and the Sichuan Provincial Key Lab on Signal and Information Processing (S2jj20110010).

References

- [1] Meng Q. A data model supporting content-based image retrieval. *Computer Applications and Software*. 2007; 24(1): 65-67.
- [2] Meenakshi M, Bowman DS, Sonali B, Death CG. *Comparison of different CBIR techniques*. 2011 3rd International Conference on Electronics Computer Technology. 2011; 4: 372-375.
- [3] Zukuan WEI, Hongyeon KIM, Youngkyun KIM, Jaehong KIM. An Efficient Content Based Image Retrieval Scheme. *TELKOMNIKA Indonesian Journal of Electrical Engineering*. 2013; 11(11): 6986-6991.
- [4] Guizhi Li. Improving Relevance Feedback in Image Retrieval by Incorporating Unlabelled Images. *TELKOMNIKA Indonesian Journal of Electrical Engineering*. 2013; 11(7): 3634-3640.
- [5] Chang WH, Cheng MC, Kuo CM, Yang NC, Huang DS. An efficient contour-based layered shape descriptor for image retrieval. *International Journal of Innovative Computing, Information and Control*. 2011; 7(7): 3903-3922.
- [6] Li XH, Shen LS. Compressed domain based image retrieval technology. *Chinese Journal of Computers*. 2003; 26(9): 1051-1059.
- [7] Lay JA, Guan L. *Image retrieval based on energy histograms of the low frequency DCT coefficients*. Proc. Of IEEE International Conference on Acoustics, Speech, and Signal Processing. 1999; 6: 3009-3012.
- [8] Lu ZM, Li SZ, Burkhardt H. A content-based image retrieval scheme in JPEG compressed domain. *International Journal Of Innovative Computing, Information and Control*. 2006; 2(4): 831-839.
- [9] Lu ZM, Burkhardt H. color image retrieval based on DCT-domain vector quantization index histograms. *Electronics Letters*. 2005; 41(17): 956-957.
- [10] Hossein N, Saeid S. *Object-based image indexing and retrieval in DCT domain using clustering techniques*. Proceedings of World Academy of Science, Engineering and Technology. 2005; 3: 98-101.
- [11] Feng G, Jiang J. JPEG compressed image retrieval via statistical features. *Pattern Recognition*. 2003; 36(4): 977-985.
- [12] Huang X, Song L, Shen L. Image retrieval based on DCT compressed domain. *Acta Electronica Sinica*. 2002; 30(12): 1786-1789.
- [13] Zhang X, Yu C. Medical image retrieval research. *Medical Information*. 2010; 23(7): 2271-2272.
- [14] Shen Y, Li M, Xia S. A survey on content-based medical image retrieval. *Journal of Computer-Aided Design & Computer Graphics*. 2010; 22(4): 569-578.
- [15] Shen L, Zhang J, Li X. *Image Retrieval and Compressed Domain Processing*. Beijing: Posts & Telecom Press. 2008.
- [16] Gonzalez RC, Woods RE. *Digital Image Processing*. Beijing: Publishing House Of Electronics Industry. 2002.
- [17] Mueller H, Mueller W, Squire Marchand-Maillet DS, Pun T. Performance evaluation in content-based image retrieval: overview and proposals. *Pattern Recognition Letters*. 2001; 22(5): 593-601.